

Adjoint analysis and control opportunities in a 2D jet

L. I. Cerviño, T. R. Bewley

Flow Control Lab, Dynamic Systems and Control Group, Dept. of MAE, UC San Diego

Abstract—Model predictive control (via adjoint-based optimization) has already been applied successfully to large nonlinear systems for which the delay between the control actuation and the resulting effect on the metric of interest is large. This method extends naturally to high-dimensional discretizations of infinite-dimensional multiscale PDE systems such as compressible turbulent jet flows, for which the dimension of the system when discretized in space can be on the order of $N \sim O(10^7)$. Such optimizations involve an expensive iterative procedure; our lab is currently gearing up to perform such supercomputer-based optimizations of 3D compressible turbulent jet systems. As an intermediate result, much may be learned from 2D adjoint calculations in this system to identify the sensitivity of the system to control actuation at various locations. The suitability of different types of control at different locations may be inferred from this sensitivity. It is seen that modification of the high-frequency noise radiated to the far field is possible with low-frequency actuation near the jet nozzle, and that mass sources are more effective than heat sources for modifying the acoustic field via forcing of the hydrodynamic field.

I. INTRODUCTION

Passive noise reduction strategies have already been explored extensively in order to reduce the noise radiated by turbulent jets, especially using techniques which reduce the convective Mach number, in the supersonic regime (see, e.g., [10]), and more recently in subsonic turbofans ([11]). Effective, unsteady, individually-controllable actuators at the exit of the nozzle have already been developed and tested (at full scale) for the problem of jet mixing enhancement, as seen in Figure 1. However, to the best of our knowledge, no active control strategy has yet succeeded for the purpose of jet noise reduction in such systems due to the complex nature of the physics involved and the high-dimensional aspect of the control forcing schedule to be optimized.

Adjoint-based nonlinear system optimization is a popular technique in the flow control community. The adjoint system, when defined and calculated appropriately, gives very accurate gradient information with which controls may be tuned even in high-dimensional systems with high-dimensional controls. The performance of a control distribution optimized via this method cannot be guaranteed to be globally optimal, but it often far exceeds that possible with other control design techniques. Adjoint-based gradient optimization has proven to be effective in the analysis, control, optimization and forecasting of incompressible turbulence (see, e.g., [1]). Recently, there has been an increased interest in extending this approach to compressible flows (see, for example [15], where a 6.3dB reduction of noise in a 2D shear layer

is obtained). The ultimate goal of the present project is to achieve 3D jet noise reduction via active control using an adjoint-based optimization procedure by optimizing the azimuthal and temporal distribution of the actuator forcing near the jet exhaust, as illustrated in Figure 1.

Due to the high cost of the optimization procedure, it is useful to perform first an adjoint analysis and to evaluate whether the type of control which we intend to apply is appropriate for this problem. The adjoint analysis reveals the sensitivity of the cost function to modification of the control actuation. Further, if an eigenvalue/eigenvector analysis is performed, it may be used to characterize the stabilizability of the system, as discussed in detail in [7]. Adjoint analysis is thus a valuable tool, since quantification of the stabilizability and the suitability of proposed actuator configurations in a large system such as that studied here is difficult to obtain without it.

For the simulation-based characterization and optimization of jet noise, it is important to obtain an accurate calculation of the hydrodynamic and acoustic fields. This is now possible with the advance numerical methods discussed in [5] and [6], upon which our present numerical code is based.

II. PERTURBATION VS. ADJOINT ANALYSES

As summarized in Figure 1, perturbation analyses, which simulate directly the effect on the flow of a perturbation to the control distribution, characterize **control**→**effect** relationships (*If I change the control here, how and where will that affect the flow?*). A representative perturbation analysis of the present system is shown in the top row of Figure 2. This analysis was obtained by the Complex Step Derivative method, which has been used broadly in the optimization literature (see, e.g., [8], [9]), and has recently been extended by our group for application to pseudospectral CFD codes ([3]). Perturbation analyses characterize the propagation of disturbances in the system as it evolves forward in time. In order to perform an extensive investigation of the effect of different control possibilities, the perturbation field must be computed once for each possible location of the actuators, since it does not give at once a global view of the sensitivity of the cost function to changes to the control distribution.

In adjoint analyses an “adjoint system” is defined and computed (by marching backward in time) in order to identify the gradient of the cost function of interest to additional control forcing of the system. As depicted in Figure 1, such analyses characterize **effect**→**control** relationships (*If I want to achieve a desired effect here, how and where should I*

apply control to the flow?). A representative adjoint analysis of the present system is depicted in the bottom row of Figure 2. Once the cost function is defined, one adjoint simulation gives at once information about the sensitivity of this cost function to control actuation everywhere in the flow domain. Thus, for the purpose of control optimization, adjoint analyses provide much more valuable information than perturbation analyses.

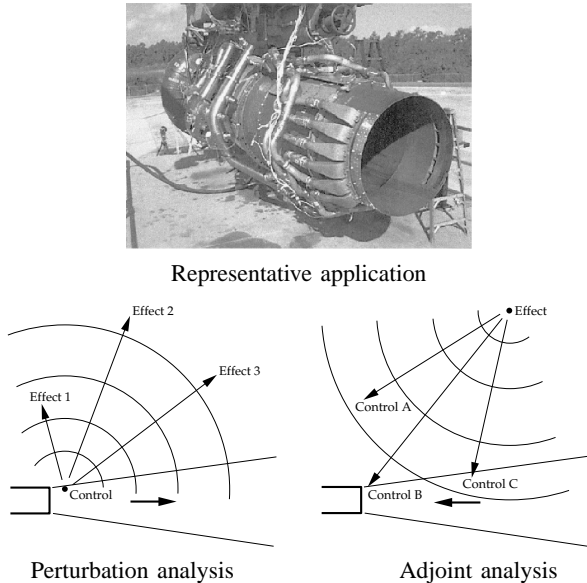


Fig. 1. Experiment by Pratt & Whitney on a JT8D engine (top); once the control forcing schedule is optimized, the actuators for the noise control problem are expected to be an order of magnitude smaller. **Perturbation analyses** (bottom left) characterize **control** \rightarrow **effect** relationships. On the other hand, **adjoint analyses** (bottom right) characterize **effect** \rightarrow **control** relationships.

It is important to note that adjoint analyses do *not* identify the “origin” or “source” of the radiated sound in such a system. Rather, they identify how and where additional forcing may be applied to the existing system to modify the radiating noise already present in a desired manner. This point is readily evident by considering a simpler model system (without the jet present), as depicted in Figure 3. Thus, identification of sound “sources” is not to be expected from adjoint analyses when applied to more complex systems, such as the unsteady jet considered in the present work.

Note that, in the remainder of the present work, the cost functions considered are essentially pointwise measures of the sound field, and the adjoint field computations are therefore referred to as “adjoint Green’s functions”.

III. DESCRIPTION OF THE SYSTEM

The system under consideration is a Mach 0.5 cold 2D jet at a Reynolds number $Re_D = \rho D U_j / \mu = 5000$ (where ρ is the density of the jet, D is the nozzle diameter, U_j is the exit velocity of the jet, and μ is the viscosity of the jet) with sinusoidal excitation near the jet exit at a Strouhal number

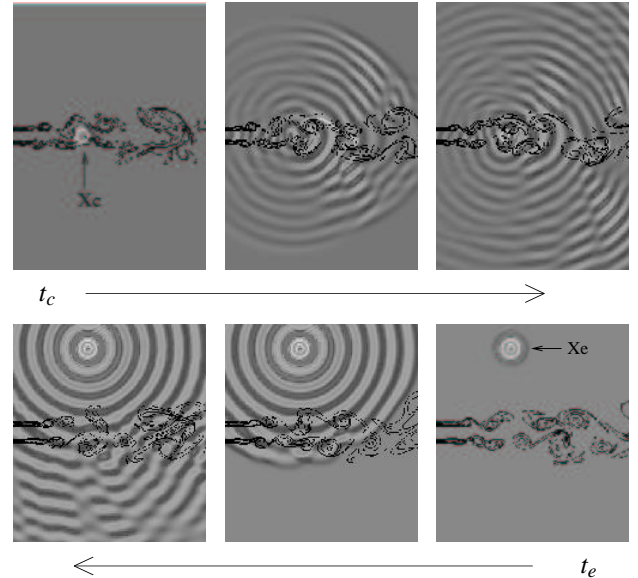


Fig. 2. **Perturbation analysis** (top) characterizes the effect on the entire flow resulting from a small change to a particular control quantity, taken here to be a sinusoidally-varying mass source at point x_c . **Adjoint analysis** (bottom) characterizes the effect on a particular flow quantity, taken here to be high frequency noise at point x_e , due to small changes in the control applied anywhere in the flow. Vorticity contours are superimposed to the colored perturbation and adjoint fields.

$St = f_0 D / U_j = 0.4$ (where f_0 is the frequency of excitation). This system is governed by the equation

$$\mathcal{N}(\mathbf{q}) = \mathbf{g}, \quad \text{where} \quad \mathbf{q} = \begin{pmatrix} p \\ \rho \mathbf{u} \\ \rho \end{pmatrix} = \begin{pmatrix} p \\ \mathbf{m} \\ \rho \end{pmatrix} \quad (1)$$

\mathbf{q} is referred to as the state field, and the operator $\mathcal{N}(\mathbf{q})$ represents the nondimensionalized full compressible Navier-Stokes equation for an ideal gas with constant specific heats c_p and c_v and constant Prandtl number Pr (for a more detailed description of the system, see [2]). Note that \mathbf{g} is the control applied, here introduced as a right-hand-side-forcing term in the governing equation. Refraction effects are expected to be significantly weaker in a cold jet than in a hot jet, as the speed of sound is identical in the ambient fluid and the jet core. In fact, in sharp contrast with the perturbation and adjoint analyses of the mean of a heated jet as considered by [14], the corresponding analyses of the refraction due to the mean of the cold jet flow studied here exhibit very little refraction. Nevertheless, as shown in this paper, the acoustic scattering due to the unsteady vortex roll-up in the present flow is quite pronounced even in this cold jet system, illustrating significant opportunities to control the hydrodynamic field (at low frequencies) in order to modify the high-frequency radiated noise.

The simulation code used in the present work implements the full compressible Navier-Stokes equation using a numerical method based closely on that developed by [5]. The

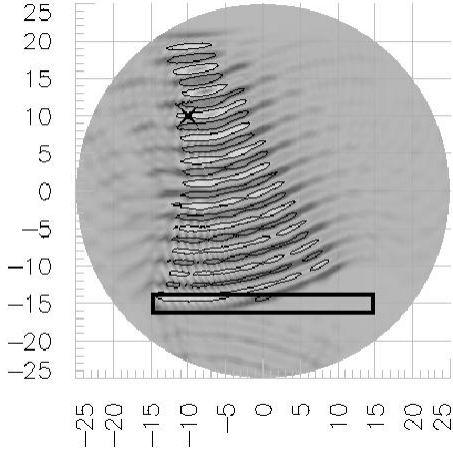


Fig. 3. Adjoint analysis of sound waves, produced by a monopole sound source at the point marked by the X, in a stationary fluid. The corresponding adjoint field is driven by the sound waves in the box and propagates away from it, as visualized above, illustrating possible locations for “antinoise” sources where additional forcing could be applied to achieve the desired effect (namely, to reduce the sound pressure level within the box). Even though the governing system represented here is a linear, constant-coefficient PDE and the cost function is quadratic in the state variables, the adjoint field identifies a range of effective “antinoise” forcing locations, and does not accurately identify the isolated sound source.

present simulations do not resolve any solid boundaries. Instead, artificial “buffer zones” have been used around the domain of physical interest, coupled with characteristic-based boundary conditions on the computational boundaries. This type of *ad hoc* but effective numerical boundary conditions simulates the effect of quiescent far-field boundary conditions on the physical system, and has now become standard for this type of problem. It is discussed further in, e.g., [6] and [4].

IV. DERIVATION OF THE ADJOINT SYSTEM

In order to develop an adjoint solver, certain additional approximations have been made, as explained in [2] (namely that the viscosity μ and the bulk viscosity of the flow μ_B are constant, and that the irreversible viscous dissipation in the energy equation is 0). These convenient simplifications are thought to be acceptable in the approximate adjoint analysis, as the spatial and temporal variations of viscosity in the system and the irreversible viscous dissipation in the heat equation both affect the dynamics of the system only at the small length scales, and are thus thought to be relatively unimportant in terms of the mechanics of sound generation. Subject to these additional assumptions, and following the established procedure for performing an adjoint analysis (see, e.g., appendix B of [1] for the case of an unsteady compressible Euler system), we may take the Fréchet derivative of the governing equation (described in full in [2]) to obtain a

linearized equation of the form

$$\mathcal{N}'(\mathbf{q}) \mathbf{q}' = \mathbf{g}', \quad \text{where} \quad \mathbf{q}' = \begin{pmatrix} p' \\ \mathbf{m}' \\ \rho' \end{pmatrix} \quad (2)$$

and \mathbf{q}' is referred to as the perturbation field. Selecting an L_2 duality pairing of the form $\langle \mathbf{q}^*, \mathbf{q}' \rangle \triangleq \int_0^T \int_{\Omega} \mathbf{q}^* \cdot \mathbf{q}' dx dt$, this linearized operator is then transformed according to the identity

$$\langle \mathbf{q}^*, \mathcal{N}'(\mathbf{q}) \mathbf{q}' \rangle = \langle \mathcal{N}'(\mathbf{q})^* \mathbf{q}^*, \mathbf{q}' \rangle + b, \quad \text{where} \quad \mathbf{q}^* = \begin{pmatrix} p^* \\ \mathbf{m}^* \\ \rho^* \end{pmatrix} \quad (3)$$

and \mathbf{q}^* is referred to as the adjoint field. The L_2 norm has been selected here, even though in multiscale PDE systems such as the present, the L_2 duality pairing is not necessarily the best choice for defining the adjoint operator, and incorporating spatial or temporal derivatives into this pairing is recognized to have an important regularizing effect on the spectra of the resulting adjoint field that must be calculated (for further discussion of this important topic, see [12]). After some algebra involving several integrations by parts, it is straightforward to obtain the adjoint operator corresponding to the approximate linearized form of the compressible Navier-Stokes equation in this framework (see [2] for details). It is important to note that, in the present derivation, we have associated the “adjoint pressure” p^* with additional forcing of the continuity equation $\partial \rho / \partial t$, and the “adjoint density” ρ^* with additional forcing of the selected form of the energy equation $\partial p / \partial t$ (this is in contrast with, e.g., the nomenclature selected by [14]).

In a domain enclosed by solid boundaries, by selecting the appropriate adjoint boundary and initial conditions, we can make the boundary term b in (3), which results from the several integrations by parts, equal to zero. Alternatively, as in the present analysis, we may surround the physical part of the domain of interest in both the flow and adjoint problems with the numerical equivalent of quiescent far-field boundary conditions which propagate no information toward the physical domain of interest; this again effectively allows us to neglect the influence of b . By so doing, the adjoint identity (3) then reveals that the following two analyses are equivalent:

#1) analyzing the effect on $q'_i(\mathbf{x}_e, t_e)$ (that is, the effect on the i 'th component of the perturbation field at point $\mathbf{x} = \mathbf{x}_e$ and time $t = t_e$) created by applying a localized force $g'_j = \delta(\mathbf{x} - \mathbf{x}_c) \delta(t - t_c)$ to the j 'th component of the perturbation equation, and

#2) analyzing the effect on $q^*_i(\mathbf{x}_c, t_c)$ created by applying a localized force $g^*_i = \delta(\mathbf{x} - \mathbf{x}_e) \delta(t - t_e)$ to the i 'th component of the adjoint equation.

By the identity (3), we may relate the perturbation and adjoint

fields in these two analyses by

$$q_i'(\mathbf{x}_e, t_e) = q_j^*(\mathbf{x}_c, t_c). \quad (4)$$

Note that the point \mathbf{x}_c and time t_c do not appear in the formulation of the adjoint system in problem #2, but arise only in the subsequent analysis of the resulting adjoint field. Thus, a *single* adjoint calculation allows us to quantify the effect of forcing *anywhere* in the flow system (for any \mathbf{x}_c, t_c , and j) on the particular flow quantity $q_i'(\mathbf{x}_e, t_e)$. This relation between the perturbation and adjoint Green's functions provides an alternative but equivalent explanation of the significance of adjoint analyses to the explanation provided in Figure 1.

V. CALCULATION OF AN ADJOINT GREEN'S FUNCTION

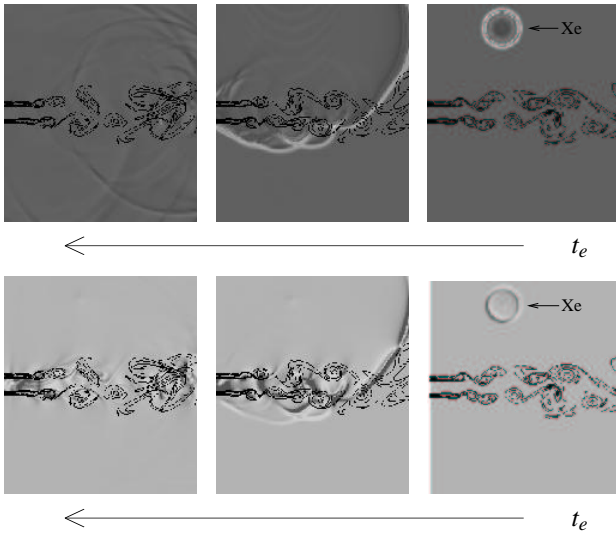


Fig. 4. Adjoint density (top) and adjoint pressure (bottom) reveals sensitivity of the pressure component of the perturbation field at point x_e at time t_e to additional control forcing in, respectively, the energy equation (top) and the continuity equation (bottom) everywhere in space x_c and for all times $t_c < t_e$. Note that, by causality, the adjoint field is zero for $t_c > t_e$; that is, the adjoint field marches backward in time from $t = t_e$.

Figure 4 illustrates a computation of the adjoint Green's function, as formulated at the end of the previous section, obtained by forcing the adjoint system $\mathcal{N}'(\mathbf{q})^* \mathbf{q}^* = \mathbf{g}^*$ with an isolated force at a particular point in space and time, that is, $g_i^* = \delta(\mathbf{x} - \mathbf{x}_e)\delta(t - t_e)$. As discussed above, each component j of the resulting adjoint Green's function, at each point in space \mathbf{x}_c and each instant in time t_c , may be interpreted as the i 'th component of the perturbation to the flow at point \mathbf{x}_e and time t_e that would arise due to localized forcing of the corresponding component j of the flow system at the corresponding point in space \mathbf{x}_c and time t_c . The calculation reported in Figure 4 takes $i = 1$, that is, the adjoint field shown characterizes the effect on the perturbation pressure $p'(x_e, t_e)$.

It is interesting to note that the disturbance in the adjoint pressure grows rapidly as it propagates within the jet toward

the nozzle at the convective velocity as the adjoint field evolves (in backward time). In contrast, the disturbance in the adjoint density essentially propagates right through the jet, experiencing significant refraction. This behavior is quantified further in Figures 5 and 6. The component of the adjoint density that propagates at the convective speed of the jet within the jet shear layers is found to be quite small. This indicates, as one might expect, that mass sources are more efficient than energy sources in modifying the hydrodynamic field in a way which changes the radiated noise.

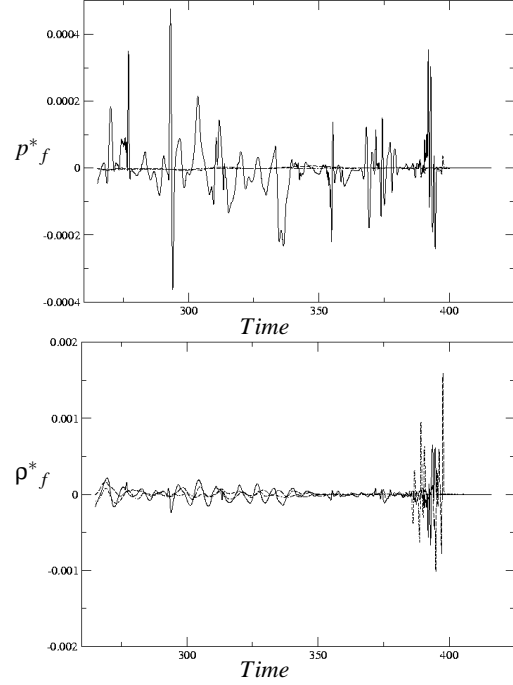


Fig. 5. Evolution of adjoint pressure (top) and adjoint density (bottom) in time at the points $\{x,y\}$ of (solid) $\{5D,0\}$, (dashed) $\{5D,2.5D\}$, (dot-dashed) $\{5D,-2.5D\}$.

VI. AN ADJOINT GREEN'S FUNCTION AT TEMPORAL FREQUENCY f CORRESPONDING TO FAR-FIELD NOISE

An alternative to forcing the adjoint problem at an isolated time t_e is to force it at a specific temporal frequency f . This corresponds roughly to looking at the sensitivity of the sound field at point x_e (at the frequency and phase selected) to additional control forcing in the governing equations. This correspondence is only approximate, however, as the system under consideration has time-varying coefficients, and therefore frequency-based characterizations of the system's response are of limited usefulness. Note that, in systems with constant coefficients, a Bode plot completely characterizes the frequency response of the system. Such a frequency-domain analysis may only be applied to the case where only the mean flow is considered. Nonetheless, an approximate characterization of this sort may still be developed for the

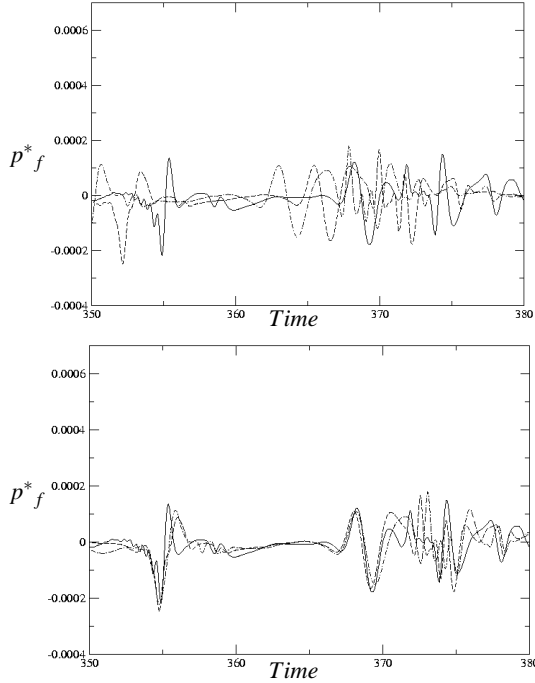


Fig. 6. Adjoint pressure at three different locations at the centerline: at (dot-dashed) $x = 8$, (dashed) $x = 9$, and (solid) $x = 10$. When the actual evolutions of the variable (top) are shifted by the time corresponding to the convection velocity (bottom), there is an approximate superposition of the three lines, which indicates that these perturbations convect toward the nozzle at the convective speed of the jet.

present system (in the time domain) simply by forcing the adjoint system sinusoidally at the frequency of interest during the backward march for the adjoint field. The computation corresponding to this kind of forcing is shown in the bottom row of Figure 2.

Instead of forcing the adjoint problem at an isolated point in the computational domain x_e we can force it along a line near the boundary of the computational domain (that is, in the “buffer zone” used to approximate the far-field boundary conditions). By so doing, one may set up a propagating wave in the adjoint field which is the same as if the computational domain extended deep into the far field and the adjoint problem was forced at an isolated point a very long distance away. By varying the forcing along this line sinusoidally, one may simulate the arrival of a wave in the adjoint field corresponding to the effect on the far-field noise in any direction of interest. A representative example is given in Figure 7. Note that both reflection and refraction of the adjoint field are observed in this computation.

VII. QUANTIFICATION OF SCATTERING OF ADJOINT GREEN’S FUNCTIONS

In an attempt to quantify the scattering of a wave in the adjoint field due to the unsteady vortex roll-up, the values of the adjoint density and adjoint pressure have been measured

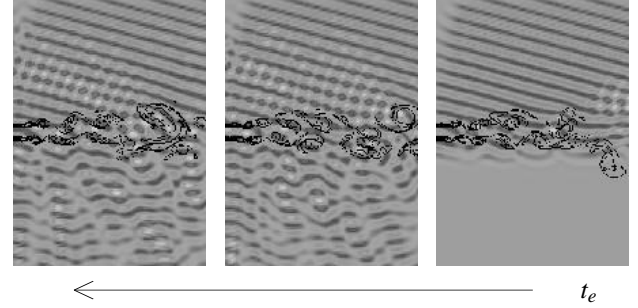


Fig. 7. Adjoint density field due to incoming waves from the far field.

at three different points in the representative adjoint Green’s function analysis illustrated in Figure 8 (top). The points where the adjoint density and adjoint pressure were measured are above the jet (where the scattering will be referred to as reflection), at the centerline, and below the jet (where the scattering will be referred to as refraction). The time series of these measurements were Fourier-transformed in time, and the results are plotted in Figure 8. The analysis was performed for adjoint forcing at two different Strouhal numbers: $St = 0.8$ ($2\times$ the vortex roll-up frequency) and $St = 2.0$ ($5\times$ the vortex roll-up frequency).

Perhaps the most important observation to make in Figure 8 is that there is very significant frequency broadening in all of the adjoint spectra measured. The adjoint systems are excited by forcing at the single frequency indicated ($St = 0.8$ or 2.0) but, due to the time-varying coefficients (from the unsteady flow field \mathbf{q}) in the adjoint operator, the measurements of the adjoint field at the points indicated exhibit energy over a broad range of temporal frequencies.

The frequency broadening present when the adjoint field is forced at a higher frequency is much larger than when it is forced at a lower frequency. This fact was noticed by [13] for the direct problem, and was described as “multiple scattering”. In the present adjoint analysis, this suggests that high-frequency noise may be modified by a broad range of possible forcing frequencies.

Note in particular that the frequency spectrum is generally narrower at the point above the jet (dashed lines) than below the jet (dot-dashed lines), apparently because the refraction of the traveling wave in the adjoint field is stronger than the reflection of this wave for the incidence angle tested. Within the jet (solid line), it is observed that the frequency broadening is strongest.

The low-wavenumber components of the spectra of the adjoint pressure at the centerline are especially strong for all three forcing frequencies tested. This indicates that low-frequency modulation of the hydrodynamic field via mass sources within the jet can have a significant impact on the high-frequency noise in the far field, and provides impetus for further studies in jet-noise control based on such characterizations to exploit this sensitivity.

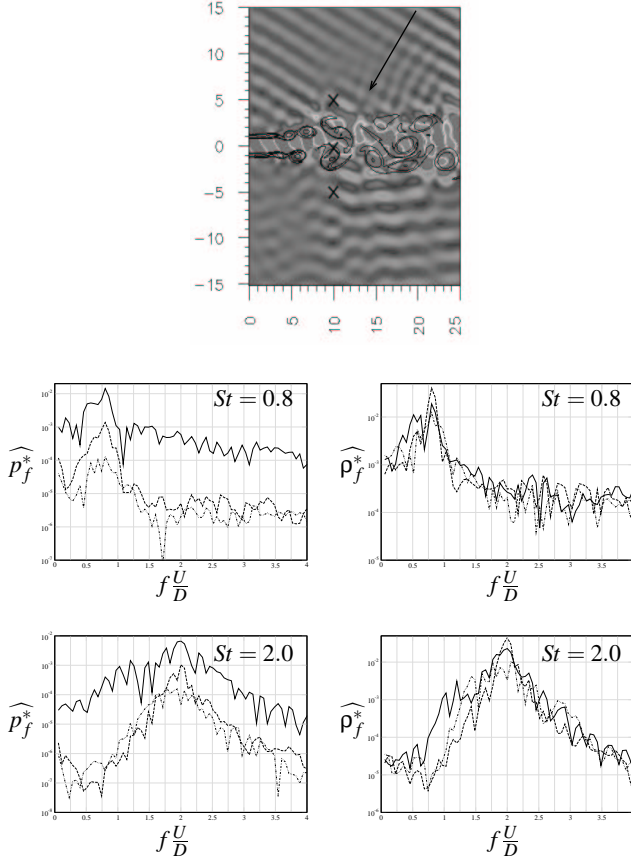


Fig. 8. Adjoint pressure wave (top) corresponding to far-field noise at an angle of 60° off the jet axis and at a frequency of $St = 2.0$, and temporal spectra measured at the indicated points $\{x, y\}$ of (solid) $\{5D, 0\}$, (dashed) $\{5D, 2.5D\}$, (dot-dashed) $\{5D, -2.5D\}$ of (left) the adjoint pressure \widehat{p}_f^* and (right) the adjoint density $\widehat{\rho}_f^*$ of incoming waves at the same angle and at a frequency of (middle) $St = 0.8$ and (bottom) $St = 2.0$.

Note also that all of the spectra are somewhat jagged, and the distance between each small peak in this jaggedness is $\Delta f = 0.2D/U$, which is exactly half of the vortex roll-up frequency. This appears to indicate (as one might expect) that the scattering of the wave in the adjoint field is closely related to its interactions with the large-scale vortex roll-up.

A second set of cases was also run in which the wave in the adjoint field approaches the jet at a 90° angle off the jet axis (cf. Figure 8). The results showed very similar trends, and are thus not included here.

VIII. CONCLUDING REMARKS

An adjoint analysis in an unsteady compressible 2D jet has been performed in order to obtain insight on control opportunities in this system. Attention has been focused on the scattering of adjoint Green's functions corresponding to far-field high-frequency noise. Significant scattering of the adjoint field is detected both above and below the jet, as quantified by a spectral analysis of the adjoint field. This

scattering is a direct result of system unsteadiness (vortex roll-up), and cannot be captured by mean flow analyses.

The degree to which frequency broadening extends into the low frequencies within the jet in the adjoint analyses indicates the degree to which low-frequency alteration of the hydrodynamic field can be used to affect the high-frequency radiated acoustic field. This distinguishes promising low-frequency “hydrodynamic” control strategies from simple (but perhaps impractical) “antinoise” control strategies, which must be applied at the frequency of the radiated noise.

The authors thank Profs. Jon Freund and Sanjiva Lele for helpful discussions and for hosting our visit to the summer program of the Center for Turbulence Research (CTR), where much of this work was performed. The authors also thank AFOSR (Dr. John Schmisser and Dr. Belinda King) for generous funding in support of this research.

IX. REFERENCES

- [1] BEWLEY, T.R., MOIN, P., & TEMAM, R. 2001 DNS-based predictive control of turbulence: an optimal benchmark for feedback algorithms. *J. Fluid Mech.* **447**, 179-225.
- [2] CERVIÑO, L.I., BEWLEY, T.R., FREUND, J.B., & LELE, S.K. 2002 Perturbation and adjoint analyses of flow-acoustic interactions in an unsteady 2D jet. *Center for Turbulence Research, Proceedings of the Summer Program 2002*, 27-40.
- [3] CERVIÑO, L.I. & BEWLEY, T.R. 2003 On the extension of the complex-step derivative technique to pseudospectral algorithms. *J. Comp. Physics.* **187**, 544-549.
- [4] COLONIUS, T., LELE, S.K., & MOIN, P. 1993 Boundary conditions for direct computation of aerodynamic sound generation. *AIAA J.* **31**, 1574-1582.
- [5] FREUND, J.B., MOIN, P., & LELE, S.K. 1997 Compressibility effects in a turbulent annular mixing layer. Mech. Eng. Dept., Stanford University, Tech. Rept. TF-72.
- [6] FREUND, J.B. 1997 Proposed inflow/outflow boundary condition for direct computation of aerodynamic sound. *AIAA J.* **35**, 740-742.
- [7] LAUGA, E. & BEWLEY, T.R. The decay of stabilizability with Reynolds number in a linear model of spatially developing flows. *Proc. R. Soc. Lond. A* **459**, 2077-2095.
- [8] LYNES, J.N. & MOLER, C.B. 1967 Numerical differentiation of analytic functions. *SIAM J. Numer. Anal.* **4**, 202-210.
- [9] MARTINS, J. R. R. A., STURDZA, P., & ALONSO, J.J. 2001 The connection between the complex-step derivative approximation and algorithmic differentiation. *AIAA Paper 2001-0921*.
- [10] PAPAMOSCHOU, D. 1997 Mach Wave Elimination in Supersonic Jets. *AIAA Paper 1997-0147*.
- [11] PAPAMOSCHOU, D. 2003 A New Method for Jet Noise Reduction in Turbofan Engines. *AIAA Paper 2003-1059*.
- [12] PROTAS, B., BEWLEY, T.R., & HAGEN, G. 2002 A computational framework for the regularization of adjoint analysis in multiscale PDE systems. In press, *J. Comp. Physics*.
- [13] SUZUKI, T. 2001 Acoustic wave propagation in transversely sheared flows. PhD Thesis, Stanford University, Department of Aeronautics and Astronautics. Also available as SUDAAR 739.
- [14] TAM, C.K.W. & AURIAULT, L. 1998 Mean flow refraction effects on sound radiated from localized sources in a jet. *J. Fluid Mech.* **370**, 149-174.
- [15] WEI, M. & FREUND, J.B. 2002 Optimal control of free shear flow. *AIAA Paper 2002-0665*.